AIAA 53rd Aerospace Sciences Conference
Kissimmee, FL

AIAA 2015-0061
Special Session on AVT-183 Aerodynamics

A Reduced-Complexity Investigation of Blunt-Leading-Edge Separation Motivated by UCAV Aerodynamics

James M. Luckring[1]
NASA Langley Research Center, Hampton, VA, 23681, USA

Okko J. Boelens[2]
National Aerospace Laboratory – NLR, Amsterdam, The Netherlands

A reduced complexity investigation for blunt-leading-edge vortical separation has been undertaken. The overall approach is to design the fundamental work in such a way so that it relates to the aerodynamics of a more complex Uninhabited Combat Air Vehicle (UCAV) concept known as SACCON. Some of the challenges associated with both the vehicle-class aerodynamics and the fundamental vortical flows are reviewed, and principles from a hierarchical complexity approach are used to relate flow fundamentals to system-level interests. The work is part of roughly 6-year research program on blunt-leading-edge separation pertinent to UCAVs, and was conducted under the NATO Science and Technology Organization, Applied Vehicle Technology panel.

I. Nomenclature

AR	aspect ratio, b^2/S	r_{le}	streamwise leading-edge radius
b/2	wing semispan	S	wing area
C_L	lift coefficient, lift / ($q_\infty S_{ref}$)	t	airfoil maximum thickness
C_m	pitching moment coefficient, pitching moment / ($q_\infty c_{ref} S_{ref}$)	U_∞	free stream reference velocity
C_p	static pressure coefficient	x,y,z	body-axis Cartesian coordinates
c	wing chord	α	angle of attack, deg.
c_r	root chord	β	angle of sideslip, deg.
c_{ref}	reference chord	η	fraction of wing semispan
M	Mach number	Λ	wing sweep, deg.
mac	mean aerodynamic chord	μ	viscosity
q_∞	free stream dynamic pressure, ½ $\rho_\infty U_\infty^2$	ν	kinematic viscosity, μ/ρ
R_{cref}	Reynolds number based on c_{ref}, $U_\infty c_{ref} / \nu$	ρ	density
R_{mec}	Reynolds number based on mac, U_∞ mac / ν		

Subscripts

le	leading edge	te	trailing edge
ref	reference	∞	free-stream reference conditions

[1] Senior Research Engineer, Configuration Aerodynamics Branch, james.m.luckring@nasa.gov, AIAA Associate Fellow.
[2] R&D Engineer, Applied Computational Fluid Dynamics, Department of Flight Physics and Loads, Aerospace Division, okko.boelens@nlr.nl.

Acronyms

AGARD	Advisory Group for Aerospace Research and Development	RANS	Reynolds Averaged Navier Stokes
AVT	Applied Vehicle Technology	RTO	Research and Technology Organization
DLR	German Aerospace Company, *Germany*	SACCON	Stability And Control CONfiguration
EADS	European Aeronautic Defence & Space Company	STO	Science and Technology Organization
NATO	North Atlantic Treaty Organization	UAV	Uninhabited Air Vehicle
NLR	National Aerospace Laboratory, *Netherlands*	UCAV	Uninhabited Combat Air Vehicle

II. Introduction

Aircraft systems continue to become increasingly sophisticated in meeting current and project performance requirements. In some cases this entails refined performance from established vehicle classes; in others it includes significantly altered or even new vehicle classes, often with expanded operating conditions. An example of the former would be the current evolution of commercial transports that incorporate advanced composite materials, refined propulsion systems, and enhanced low-drag shaping. Examples of the latter would include the current generation of maneuvering aircraft (e.g., F-22 and F-35) as well as a suite of Uninhabited Air Vehicles (both UAVs and UCAVs).

In the case of Uninhabited Combat Air Vehicles, the combination of vehicle shaping and maneuver envelope can often produce separation-induced leading-edge vortex flows. The full systems integration for these vehicles has resulted in a new vehicle class, and the vortical flows on this vehicle class, including those separating from smooth surfaces, are likely to be quite different from those of past experiences. This presents a wealth of new aerodynamic challenges, not only as regards the full systems performance of these new vehicles, but also as regards the more fundamental flow physics of the vortical flows underlying the systems performance of this vehicle class. The connectivity of the full systems level performance with more fundamental underlying flow physics that significantly affect this performance can be a challenge in and of itself.

Several research projects to expand our understanding of UCAV aerodynamics have recently been coordinated through the Science and Technology Organization (STO) and its predecessor incarnation, the RTO, under the auspices of NATO. Among these, two projects under the oversight of the Applied Vehicle Technology (AVT) Panel within the STO form the basis for the present work. The first, "Assessment of Stability and Control Prediction Methods for NATO Air & Sea Vehicles," Task Group AVT-161, was primarily focused on dynamic stability characteristics of a UCAV concept known as the Stability And Control CONfiguration (SACCON). The second, "Reliable Prediction of Separated Flow Onset and Progression for Air and Sea Vehicles," Task Group AVT-183, was focused on one particular phenomenon from the SACCON configuration, the onset and progression of blunt-leading-edge vortex separation, and this focus was established in a way so that the more fundamental AVT-183 work, with a 53° swept diamond wing, would be relevant to the more complex AVT-161 SACCON configuration. Results from the AVT-183 research are just now being reported, and an overview of the AVT-161 research has been published by Cummings and Schütte [1] [2012].

The intent for this paper is to present the approach that was adopted to connect these two AVT projects. First, some of the aerodynamic challenges associated with UCAV configurations are briefly reviewed at a full systems level. This is followed by a brief review of the vortex flows that affect the UCAV configuration aerodynamics, but at a fundamental unit-problem level. These provide the context to the AVT-161 and the AVT-183 research projects.

Next, a hierarchical framework is applied for interconnecting not only the two AVT projects but also the broader systems and unit-problem contexts. After touching upon the collaborative approach to the work, the scope of a reduced order complexity problem is established for the problem at hand. Details of the actual design process for the reduced order problem are given by Boelens[2] et al. [2015], and outcomes from an integrated experimental[3,4] and numerical[5-12] research campaign will be reported in subsequent papers.

III. Some Complexities Associated with UCAV Aerodynamics

In this section, some aerodynamic challenges associated with a flight system are first reviewed. Vortex flow complexities at a fundamental or unit-problem level are reviewed next. Finally, the manifestation of these flows on the SACCON configuration is presented. Emphasis is placed on separation-induced leading-edge vortex flows and includes a suite of other vortical complexities associated with practical UCAV shaping practices.

A. Systems Level Aerodynamic Complexities

UCAV systems represent a new vehicle class with a number of design features that have established some new aerodynamic challenges. These challenges arise from design trades among competing constraints from propulsion–airframe integration, observables, and aerodynamic performance to name a few. This has resulted in vehicles with the aerodynamic challenges that arise not only from the new geometries but also from new or altered operating conditions.

A couple examples are shown in **Figure 1**, using the nEUROn (developed collaboratively among six European countries) and the Northrop-Grumman X47-B. Both vehicles show the propulsion-airframe integration feature of having the inlet directly behind and above the wing apex. Leading-edge vortices would normally originate from this region at maneuver conditions, and now the inlet effects could be expected to fundamentally alter this feature.

Wing leading-edge sweep angles are high enough to induce leading-edge vortex separations at maneuver, but lower than traditional slender wing values. At these sweep values adverse vortex breakdown effects can occur at angles of attack close to practical maneuver values. In general, much less is known about this class of vortex flow.

The moderate leading-edge sweep and associated moderate aspect ratios for this vehicle class result in closely coupled aerodynamics but with some alterations as compared to current maneuvering aircraft. For example, leading-edge vortex separations will occur in close proximity to the thick and blended centerbody, controls could couple with these vortices in new ways and, in some cases, the controls could couple with the exhaust in ways that differ from conventional propulsion-airframe integration practices.

(a) nEUROn, Λ_{le} = 58°

(b) X-47B, Λ_{le} = 55°/30°

Figure 1. UCAV systems operations.

These vehicles must also perform in complex operating conditions. Because the vehicles are uninhabited, the maneuver envelope can be expanded to higher-g conditions (and higher angles of attack), and this could result in leading-edge vortex characteristics not typically encountered with prior maneuvering aircraft. Carrier-based operations still require some of these new vehicles to penetrate the air ship wake in the course of carrier landing, and the altered aerodynamic characteristics of these vehicles could affect this interaction. (The photograph shows the first successful arrested landing of a tailless autonomous UCAV on a modern aircraft carrier, the USS George H. W. Bush, in summer 2013).

The two vehicles shown in Figure 1 are quite different from each other, and other variations can be found within the UCAV class of flight systems, perhaps in association with the newness of this class. However, all of these concepts incorporate moderate leading-edge sweep values and small leading-edge radii. Both the moderate sweep and blunt leading edge can significantly alter the separation-induced leading-edge vortical flows from those that occur on slender sharp-edged wings. The next section will review some of the fundamentals of separation-induced vortex flows.

B. Fundamental Vortex Flow Complexities

Here some basic attributes of separation-induced leading-edge vortex flows are reviewed, first for slender sharp-edged delta wings then for delta wings with blunt leading edges. Each of these phenomena still has unique challenges, not only in our understanding and modelling of underlying fundamentals and flow physics, but also in their manifestation on complex vehicle systems.

1. Slender wing, sharp edge

Primary and secondary vortices. At essentially any non-zero angle of attack separation is forced to occur at the sharp leading edge and for the slender wing this separation rolls up to form a stable primary leading-edge vortex. A sketch (Stollery, from Anderson[13] [1991]) is shown in **Figure 2** that illustrates these vortices. The primary vortex induces significant spanwise flow on the wing upper surface resulting in a suction peak from this vortex. Past the primary suction peak an adverse spanwise pressure gradient induces separation of the spanwise boundary layer flow resulting in a secondary separation and secondary vortex. The secondary vortex is counter rotating with respect to the primary vortex and can induce further suction outboard of the primary vortex suction peak. The primary and secondary vortices have tightly coupled interactions, and factors affecting the secondary vortex (e.g., if the secondary separation is laminar or turbulent) also affect the primary vortex. Experiments from Hummel[14] [1979] have demonstrated that when the secondary vortex was diminished, the primary vortex moved outboard and its suction peak increased.

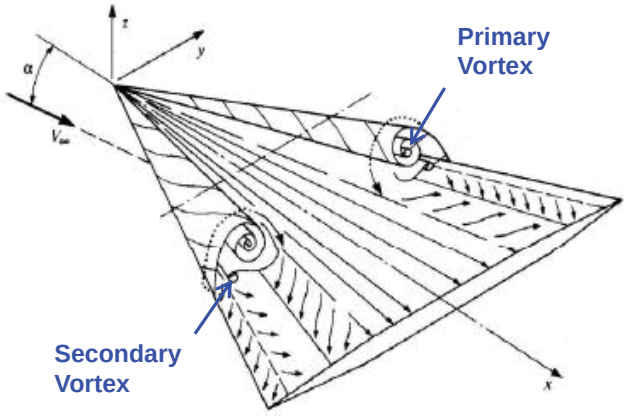

Figure 2. Primary and secondary vortices. Sharp-edged delta wing. Stollery/Anderson[13] [1991].

Vortex Breakdown. The discussions above addressed coherent leading-edge vortices. As angle of attack increases, the leading-edge vortex gains strength until, at some angle, the vortex becomes incoherent, or bursts, in the vicinity of the wing trailing edge. With further increases in angle of attack, the burst point progresses upstream, over the wing, with significant effects on wing aerodynamic characteristics such as lift, pitching moment, and buffet. Similar trends occur as leading-edge sweep is decreased.

An example is shown in **Figure 3** from the well-known results of Lambourne and Bryer[15] [1962]. The results show vortex breakdown occurring around 60% to 70% root-chord station over a 65° flat delta wing with a sharp leading edge and illustrate two modes of breakdown; a nearly axisymmetric breakdown on the port semispan and a helical breakdown on the starboard semispan. Little effect of Reynolds number on vortex breakdown characteristics for slender sharp-edged wings has been shown. Vortex breakdown, and the tantamount burst vortex flow physics, represents another class of vortex flows that, to this day, is insufficiently understood. Measurements in the vicinity of breakdown are very difficult to perform, the relationship of current turbulence models to the (unmeasured) breakdown flow physics is uncertain, and in many wing/vehicular applications the region of vortex breakdown is under resolved by the field grids. Furthermore, it appears to be an inherently unsteady phenomenon. A recent status of data sets and CFD predictions pertinent to vortex breakdown on slender delta wings was

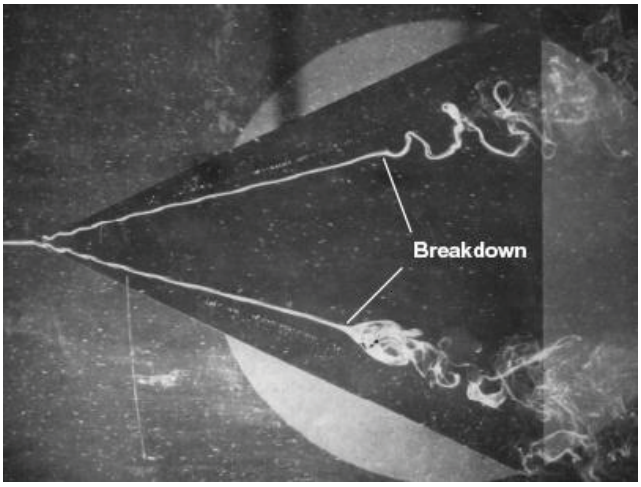

Figure 3. Vortex breakdown. Λ_{le} = 65°. Lambourne and Bryer[15] [1962].

reported[16] in 2009 by RTO Task Group 080, entitled "Vortex Breakdown over Slender Delta Wings". Eight experimental cases were catalogued, and ten CFD approaches were included, with a particular focus on a 70-degree sharp-edged delta wing experiment performed by Mitchell[17] [2003].

Vortex-vortex interactions. The coexistence of the primary and secondary vortices described above is one example of interacting vortical flows. In that case, the two vortices are counter rotating, the secondary vortex is smaller and weaker than its parent primary vortex, and the two vortices tend to stay in the relationship as described.

A second class of vortex interactions comes about between two primary vortices that are corotating. This can arise, for example, from double delta wings due to the sudden change in leading-edge sweep. Another example from a basic research configuration is shown in **Figure 4** from the work of Hall[18] [1998]. This model had a sharp chined forebody and sharp-leading-edge wing (Λ_{le} = 60°). Both sharp edges generate vortices, and the chine vortex is torn at the chine-wing juncture and persists over the wing.

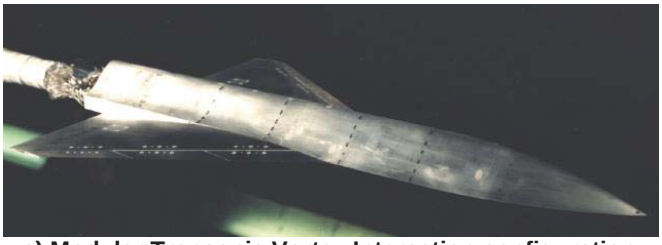

a) Modular Transonic Vortex Interaction configuration.

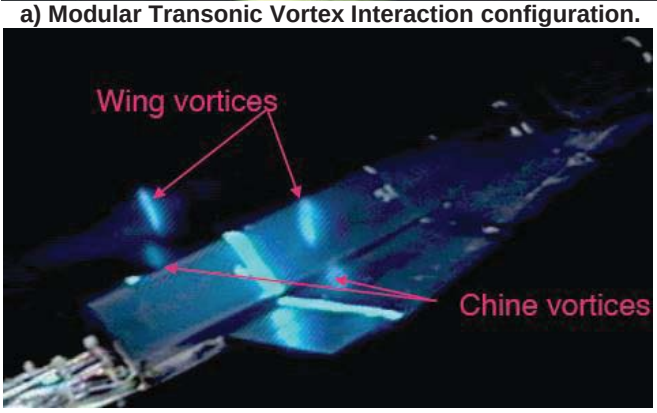

b) Interacting vortical flows.
M = 0.4, R_{mac} = 2.6 x 10^6, α = 22.5°.
Figure 4. Corotating leading-edge vortices. Hall[18] [1998].

Whereas the counter rotating primary and secondary vortex flows tend to take on a single state, corotating vortices can take on several states depending upon the relative strength and proximity of the vortices. At low angles of attack, the vortex interactions are weak and the vortices can each track somewhat independently over the body and wing, but as angle of attack increases, the vortices become stronger and more closely situated to each other. The induced effects will certainly alter the vortices (as compared to isolated vortex characteristics), and at some critical angle of attack, the strong interactions between the vortices can result in the outer vortex lifting off the wing surface and braiding around the inner vortex while the inner vortex is mutually induced outboard over the wing. An example of this interaction is shown in Figure 4b at a station slightly ahead of the wing trailing edge. Here the vortex interaction has displaced the wing leading-edge vortex upward and inboard of the chine vortex, which has been displaced outboard over the wing. Needless to say, vortex breakdown characteristics can be significantly altered by such vortex interactions.

Finally, it is noted that each of the primary leading-edge vortices of necessity has its own secondary vortex as described above. Once again, secondary separation affects the primary vortex strength and location, and hence secondary separation would affect the interaction between the corotating primary vortices.

Shock-vortex interactions. Although shock waves constitute a separate class of flow structures, it would be remiss not to briefly address shock-vortex interactions. A number of supersonic shock-vortex interaction domains have been established by Miller and Wood[19] [1985], expanding the earlier work of Stanbrook and Squire[20] [1964], and an example from one domain is shown in **Figure 5**. The image is a full-span cross-flow plane vapor screen as seen looking upstream from a position aft and above a 75° swept sharp-edged delta wing. In addition to the leading-edge vortices, a curved cross-flow shock can be seen atop of each vortex. There is also a shock spanning the two vortices, slightly above the wing. Six different supersonic domains distinguishing shocks, vortices, and shock-vortex

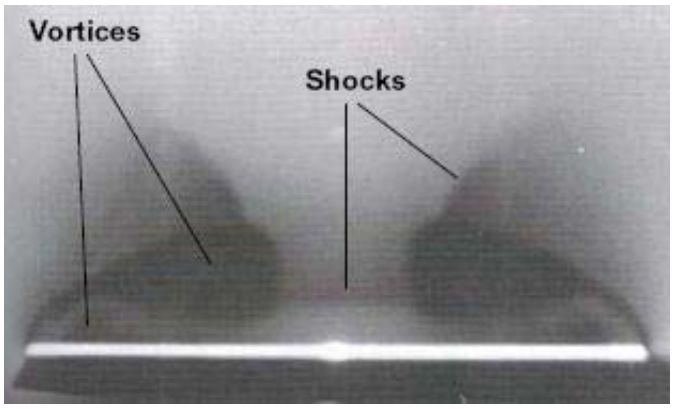

Figure 5. Supersonic shock-vortex interactions.
Λ_{le} = 75°, M = 2.4, R_{mac} = 2.5 x 10^6, α = 20°.
Miller and Wood[19] [1985].

interactions were identified by Miller and Wood in terms of the Mach number and angle of attack normal to the delta wing leading-edge sweep. The underlying shock-vortex flow physics could differ among these domains.

Transonic shock-vortex interactions are entirely different, and discussions of shock-vortex interactions as regards vortex breakdown can be found in the work from Schiavetta[21] [2009].

2. Slender wing, blunt edge

All of the vortex phenomena discussed thus far are fundamentally altered by changing the leading edge from sharp to blunt. With the blunt leading edge, the flow can be fully attached at low angles of attack, and as angle of attack increases the origin of vortex separation will first occur at the wing tip and then progress up the leading edge.

An example is shown in **Figure 6** with recent experimental results from Konrath[22] [2008]. The measurements show the vortex separation occurring about half way down the leading edge, and also show a fundamentally altered structure to this blunt-leading-edge vortical separation. After a protracted region of incipient separation near the leading edge, a second inner vortex is spawned in association with the outer primary leading-edge vortex separation. These vortices are corotating.

This new flow structure appears for the separation-induced leading-edge vortical separation from a blunt leading edge; it is fundamentally different from the sharp-edged case. In addition, all the previously discussed vortex phenomena with the sharp leading edge are modulated by the blunt leading edge. For example, vortex position and strength are altered with the blunt leading edge, so vortex breakdown and vortex interactions will be different. Moreover, shifts in load distributions associated with the part-span vortex separation contribute induced effects that further alter the blunt-leading-edge vortex from the more familiar sharp-edged full-span case.

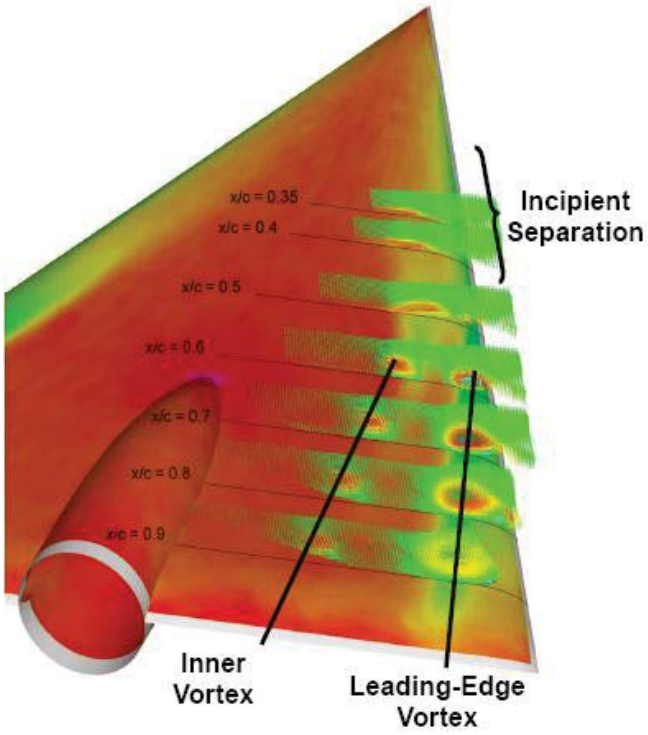

Figure 6. Blunt-leading-edge vortex separation. Λ_{le} = 65°, M = 0.4, R_{mac} = 3 x 10^6, α = 13.3°. Konrath [2008].

Finally, Reynolds number has significant effects on these flows as regards the blunt-leading-edge separation as discussed by Luckring[23] [2004]. An increase in Reynolds number will delay the onset and progression of the blunt-leading-edge separation. In the same work, Luckring shows that an increase in Mach number will promote this separation. These Mach and Reynolds number effects are absent for the sharp-edged wing. Additional discussions of factors affecting blunt-leading-edge separation can be found in Luckring[24] [2010].

3. Summary Status

As a summary to these fundamental vortex flows, it is useful to assess which among them can be considered as having something we might consider as validated CFD prediction capability. Some of the questions to consider include:

- Do we understand the critical flow physics underlying a particular flow phenomenon?
- Do we understand how to numerically approximate these critical physics (e.g., turbulence models, grid resolution, temporal effects, etc.)?
- Do we have fundamental data to validate any such resultant numerical simulations?
- Do we understand how these critical physics might be affected from ground to flight scales?

Such a list could be longer and have more detail, but the underlying principle here is to get the right answer for the right reason. A validated numerical outcome may match or miss an experimental outcome depending upon whether the simulated physics replicate the critical experimental physics or not.

The authors have assembled a snapshot of the validation status for the vortex flow topics briefly discussed in Section III-B-2, and this is presented in **Table 1**. There has been a wealth of research that has continued to advance our understanding among all these topics, and of course the literature is full of comparison assessments between various numerical methods and experiments. None the less, most of the vortical flows listed lack a validated prediction capability, even for sharp-edged delta wings. The few cases that perhaps are validated can trace much of this status to the exceptionally detailed and thorough experimental results performed by Hummel[14] [1979]. The list is by no means exhaustive (e.g., dynamic effects have not been addressed). The manifestation of these flows on full systems-level vehicles is all the more daunting.

Table 1. Validation status, some fundamental vortex flows.

Vortex Flow Topic, static conditions	Physics Understood?	Validated CFD?
Sharp edge, slender wing, primary	yes	probably
Sharp edge, slender wing, secondary	yes	possibly
Vortex Breakdown	possibly	no
Vortex tearing	no	no
Vortex-vortex interactions	no	no
Shock-vortex interactions	no	no
Blunt leading edge, vortex onset/progression	no	no
Blunt leading edge, inner vortex	no	no

These vortex examples have been purposely anchored within slender-wing aerodynamics. The high sweep angles are conducive to the formation and subsequent study of separation-induced leading-edge vortex flows. This class of wing still affords many opportunities to advance our understanding of these vortex flows.

Practical wing design considerations however result in lower leading-edge sweep values and higher aspect ratios than the more traditional slender-wing (cf., Section III-A). Such wings with moderate sweep and aspect ratio can be referred to as semi-slender wings. The semi-slender wing is very challenging for wing design and analysis in that it can be unclear to what extent either slender-wing or high aspect-ratio-wing principles apply. UCAV configurations fall in this category as well as maneuvering aircraft, **Figure 7**. The fundamental vortex properties just described will be altered in these circumstances.

From the slender wing perspective, two effects are noteworthy. First, as sweep is decreased, the leading-edge vortex strength will increase. (See Hemsch and Luckring[25]). Among other consequences, this means that vortex breakdown will occur at lower angles of attack, in association with the lower sweep, and thus potentially impact more of the practical angle of attack range. Second, the trajectory of the leading-edge vortex is at a greater angle to the free stream direction for the semi-slender wing. This can increase spanwise vortex curvature over the wing (departing from slender wing aerodynamics) and potentially entice multiple spanwise vortex structures.

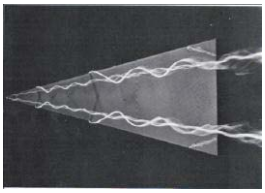

Slender wings
- High sweep, low aspect ratio
- Similarity in crossflow plane
- Cross-plane aerodynamics modulated by longitudinal load

Semi-slender wings
- Moderate sweep and aspect ratio
- Similarity?
- Application of high-AR or slender-wing principles less clear

High aspect-ratio wings
- Low sweep, high aspect ratio
- Similarity in streamwise plane
- Airfoil aerodynamics modulated by span load

Figure 7. Semi-slender wings.

Much less is known about the separation-induced leading-edge vortices for these semi-slender wings than for the more highly swept slender wing. A brief look at how some of these features are manifested on the SACCON configuration is presented next.

C. Parent Problem - SACCON

Systems-level vehicular complexities are often reduced for research and development purposes, and one such case led to the UCAV configuration SACCON. Here the SACCON configuration and aerodynamics are briefly reviewed with a focus on the complex vortical flows that are still present on this configuration.

1. Configuration

The SACCON configuration was designed by EADS and DLR to capture many aspects of UCAV aerodynamics while at the same time being suitable for international collaborative research. The configuration has an edge-aligned lambda-wing planform with a constant-chord outer panel, a leading-edge sweep of 53° and an aspect ratio of approximately 3.1, **Figure 8**. A number of systems-level features were eliminated for this configuration. For example, there was no inlet or exhaust on the model and control surfaces were excluded from the initial work. SACCON could be considered a subsystem to a full systems-level vehicle such as those discussed in Section III-A.

Figure 8. SACCON configuration in the Low-Speed Wind Tunnel, Braunschweig Germany (DNW-NWB). Λ_{le} = 53°.

A number of systems-level features were represented with SACCON. These included fairly complex spanwise distributions of thickness and leading-edge radius, **Figure 9**. The centerbody is very thick, and the thickness-to-chord ratio diminishes in the spanwise direction. The leading edge is essentially sharp from the apex out to the first trailing-edge break at which point it rapidly increases to a maximum value and then diminishes spanwise. In general, the leading-edge radii are less than 0.23% of the SACCON reference chord. The wing also includes a linear twist distribution outboard of the first trailing-edge break. The outboard twist delayed separation onset effects to higher angles of attack than would have been realized by a planar wing.

2. Aerodynamics

At low to moderate angles of attack, the attached-flow design objective was achieved. However, subsequent vortical separation was very complex. A CFD example from Frink[26] [2010] is shown in **Figure 10** for the low and moderate angle of attack conditions. Numerous vortices occur in the higher angle of attack solution and can be inferred from the surface flow patterns.

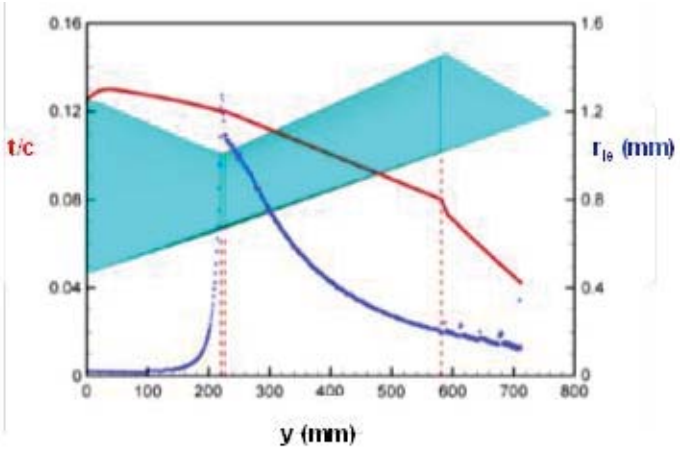

Figure 9. Some geometric complexities of SACCON, from Cummings and Schütte[1] [2012].

A sharp-leading-edge vortex is generated from the inboard portion of the leading edge, and seems to have its origin at the wing apex. The outboard portion of the wing has a blunt-leading-edge vortex, and the origin for this vortex will of course vary with angle of attack. Ahead of the blunt-leading-edge vortex is a region of attached flow near the leading edge, with some form of incipient separation flow physics as discussed earlier. The scale of the incipient separation flow physics is too small to see details in the figure.

Two other vortices are indicated in Figure 10b. Additional solution analysis has indicated an inner corotating vortex associated with the blunt-leading-edge separation as previously discussed in section III-B-2. The less-familiar thickness vortex has been identified in flow topological analysis of the SACCON configuration by Schütte[27] et al. [2012] and its likely location also identified in Figure 10b. Several secondary vortices should also be present. All of

these vortex phenomena are interacting at the conditions shown; essentially none of these phenomena, even in isolation, can be predicted with confidence using CFD.

The conditions of Figure 10b also correspond to very nonlinear force and moment characteristics, **Figure 11** (Frink[26] [2010]). Pitching moment nonlinearities actually begin around 10°, and the numerous breaks in the experimental data trends have been traced to various vortex flow effects (see Schütte[27] et al. [2012]). The scatter among various CFD results is also shown at the angles of attack for the complex vortex flows and interactions. Successful modeling of the vortical effects would be useful for predicting systems-level performance. Of course, it should be recalled that a primary focus for the AVT-161 work was dynamic stability derivatives, so the extent of flow complexity described under static conditions will be further exacerbated at dynamic conditions.

Among the contributions from the SACCON research has been the identification of remaining challenges and limitations of current CFD methods for the prediction of UCAV configuration aerodynamics. Many of these regard the multiple vortex flow phenomena that are occurring on the SACCON configuration especially in the moderate-to-high angle of attack region where the scatter among CFD results is large.

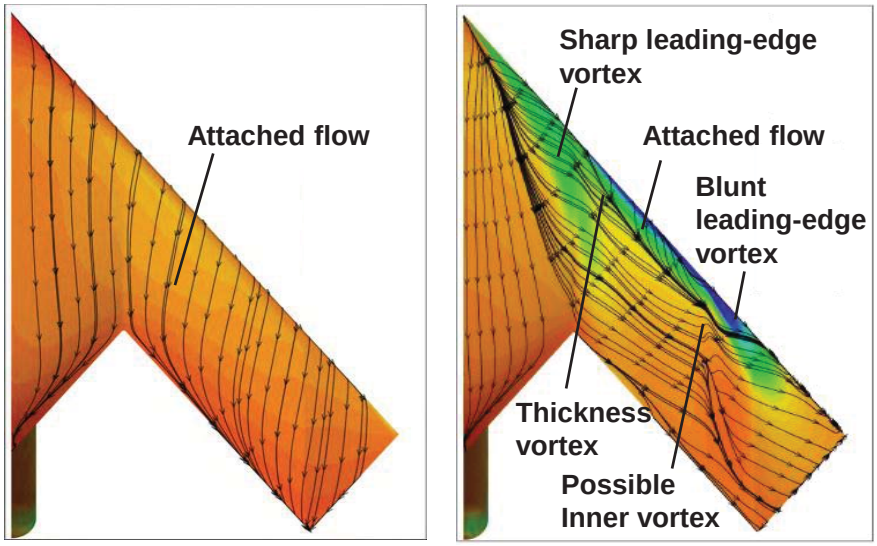

a) α = 5.28° **b) α = 16.83°**

Figure 10. Complex SACCON vortex flow phenomena. USM3D/SA, M = 0.15, R_{cref} = 1.61 x 10^6.

Given the complex nature of the vortical flows about the SACCON configuration, the current work was undertaken to isolate, as much as possible, one critical aspect of these flows in such a manner as to help discriminate why various CFD formulations differ as to their predictive capability. The phenomenon chosen for this reduced-complexity investigation was the onset and progression of blunt-leading-edge separation on the outboard portion of the wing. The location of the outer vortex is critical to any subsequent vortex interactions with the SACCON apex vortex. The location of the outer vortex separation also fundamentally affects the outer vortex strength and, hence, any manifestations of vortex breakdown. As such, successful modeling/prediction of the blunt-leading-edge vortex would be a prerequisite to modeling of other SACCON-relevant vortex phenomena (e.g., vortex interactions or vortex breakdown) and their associated aerodynamic effects.

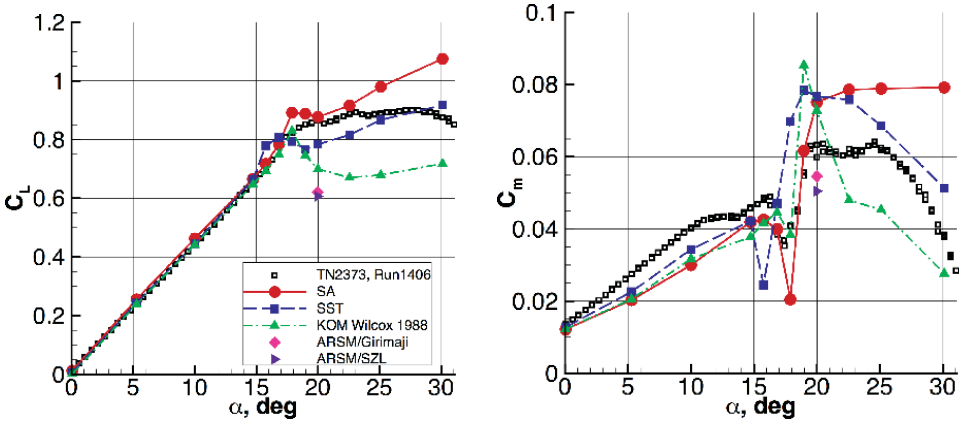

(a) Lift coefficient **(b) Pitching moment coefficient**

Figure 11. SACCON force and moment characteristics. USM3D/RANS, M = 0.15, R_{cref} = 1.61 x 10^6. Frink[26] [2010].

The simpler configuration for the present work became a particular diamond wing as described in a subsequent paper by Boelens[2] et al. [2015]. Connections among systems-level performance, subsystem investigations, and the reduced complexity investigation were viewed in terms of a complexity hierarchy.

IV. Hierarchal Decomposition of Problem Complexity

Advancements to our knowledge of complex flow phenomena pertinent to practical configurations can benefit from investigations at differing representation levels of vehicular and flow complexity. These investigation levels span from assessments of the complete vehicular system at intended operating conditions to fundamental unit-problem studies. The establishment of a problem complexity hierarchy is certainly not new (see Oberkampf and Trucano[28] [2002]), and for this work we draw upon the recent publication by Thacker[29] [2008] as well as the ASME verification and validation guide[30] [2006]. It has been demonstrated by Thacker[29] [2008] among others that roughly four representation levels can suffice to span this notional domain from complete system assessments to fundamental studies. As the level system complexity is reduced, underlying flow physics become more isolated, and hopefully elucidated. It is, of course, important that the investigations among these various levels of configuration and/or flow representation be carefully coupled for relevancy.

An example in terms of the current research interests of this paper is shown in **Figure 12**, retaining the 4-level architecture. The nEUROn has been chosen to illustrate a full system level of configuration development, and the configuration aerodynamics will be very complex and integrated as discussed in Section II-A. Full systems-level assessments tend to be better at explaining what the performance is than at explaining why the performance is as it is. The SACCON configuration has been chosen for an example of the subsystem level of the hierarchy as discussed in Section II-C. While focused on wing aerodynamics, the flow is still remarkably complex.

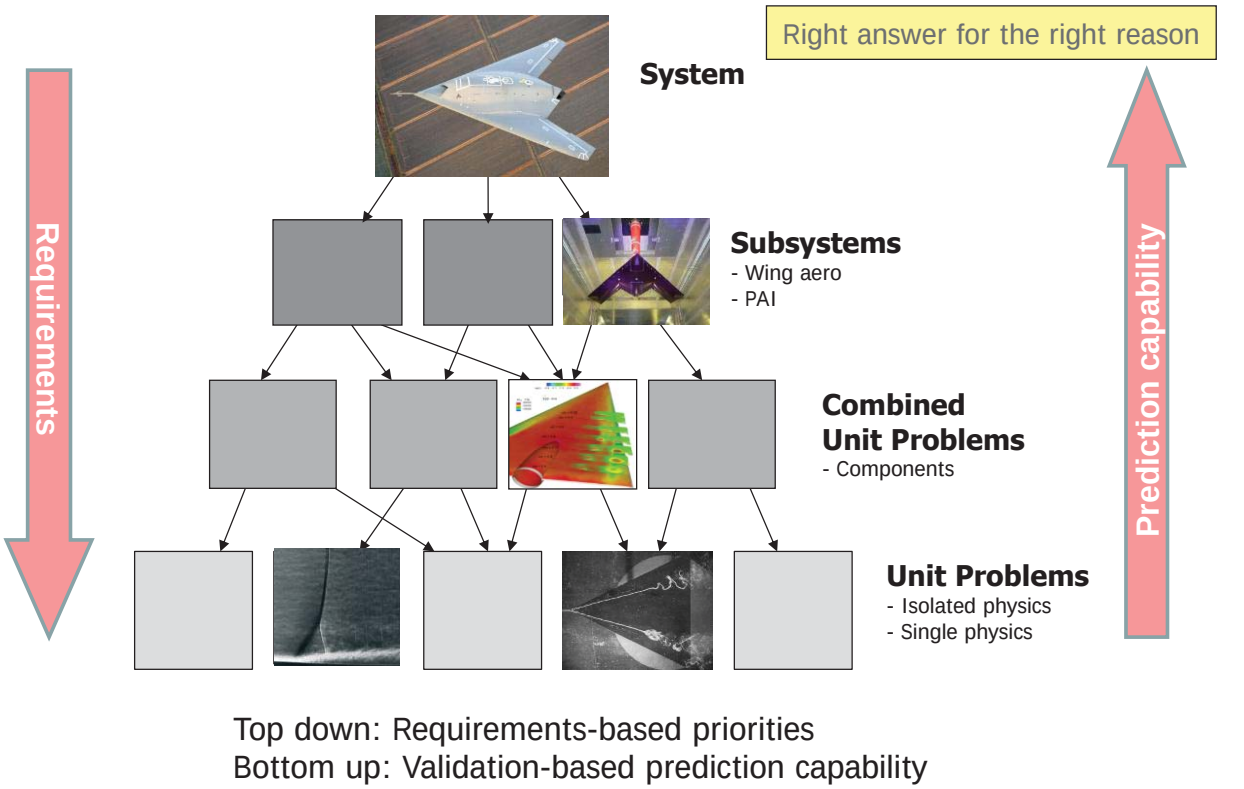

Figure 12. Hierarchical decomposition for aerodynamic complexity.

Jumping to the lowest level of the hierarchy, we find unit problems such as vortex breakdown (Section II-B) or perhaps basic shock-boundary-layer interaction. At the unit problem level, we isolate a single phenomenon to the greatest extent possible and in a manner such that the physics of interest are dominant in the overall flow. Combined unit problems occur either as a means to understand an interaction among a small number of unit problems or as a consequence of inability to further isolate combined unit effects. Unit or combined-unit problems are designed to understand why results occur as they do. Understanding what the fundamental results mean to systems level performance is accomplished through the hierarchy.

Thus, the hierarchical approach provides a rational means for spanning the domain between systems level vehicle performance and fundamental unit problem studies. Requirements flow down the hierarchy. That is, problems are identified and priorities are established from the Systems level, and they are used to inform the lower levels of the hierarchy in such a way as to help select the more basic work that will be done at unit levels of complexity. This flow down of priorities can be done heuristically or with more formal methods such as a Phenomena Identification and Ranking Table (PIRT) as reported by Wilson[31] [1998].

The unit-problem work then can help understand key flow features in a way that is relevant to higher program needs. The improved modelling at this level can then propagate up the hierarchy with step-by-step assessments for the increased configuration and flow complexities and on a path targeted at the specific system performance issue of interest. This flow up is now anchored in validation-based principles and can perhaps draw on sensitivity analyses to result in better informed predictions at the higher levels.

Successful execution of the hierarchical process will yield improved technical processes whose outcomes will model the targeted physical phenomenon at systems-level conditions for the system metric of interest. This has been referred to by some as 'the right answer for the right reason.' Of course, this outcome may or may not replicate the system metric. If you got the physics right, the improved technology should better replicate the system performance; if you did not get it right, the mismatch tells you that something else is going on. Either outcome is valuable. The objective is to understand what you have, not to match an experiment.

V. AVT-183 Diamond Wing Investigation and Collaborations

The hierarchical perspective led to the establishment of a reduced-complexity investigation of blunt-leading-edge separation motivated by UCAV aerodynamics. A design activity was undertaken to develop this unit or combined-unit investigation in such a way that (i) the work could focus on the one particular phenomenon (blunt-leading-edge separation onset and progression), and to do so in a manner that would relate to the parent configuration, SACCON.

Studies such as the present one can often require broad participation among multiple scientific institutions, not only to establish sufficient scientific numerical and experimental research diversity, but also to establish the numerical and experimental resources required for the work. In the present work, this was accomplished through the STO, and a few aspects of this collaboration are presented next.

A. Collaboration, Science and Technology Organization

The STO has proven to be a highly effective organization to facilitate collaborative scientific and technical projects of mutual interest among member countries of NATO and its affiliates. The origins of this organization go back to the Advisory Group for Aerospace Research and Development (AGARD), founded by Theodore von Karman in 1952. In 1996 AGARD was reorganized to create the RTO, and some further reorganization led to the STO (from the RTO) in 2012. During its time, the RTO was the largest such collaborative body in the world, embracing 26 NATO nations, 38 NATO partners, and over 3000 scientists and engineers. The STO has sustained this distinction, and throughout the reorganizations the STO/RTO has stayed true to the AGARD objective, namely: *to promote and conduct co-operative scientific research as well as the exchange of technical information of mutual benefit amongst NATO member nations and organizations*.

The STO facilitates various types of collaborations, and the type of interest to the present work is a Task Group. Task Groups work on a technical project for approximately four years. AVT-161 and AVT-183 are two examples of Task Group activities. The primary outcome from a Task Group is a formal technical report such as Reference 16 (Vortex Breakdown). Of course, another outcome from such work is the mutual education realized over four years or so of collaboration among the task group participants. Task Groups can establish the diversity and critical mass of expertise and resources necessary to address their project, and an example for the AVT-183 diamond wing project follows.

The business model for the STO also creates the opportunity for leveraging among the various STO-sponsored activities. With regard to the current AVT-183 project: (i) initial computational work was built upon the Vortex Flow Experiment 2 results[32,33] from the AVT-113 Task Group, "Understanding and Modeling Vortical Flows to Improve the Technology readiness Level for Military Aircraft", (ii) the hierarchical perspective for interconnecting the projects was drawn from the AVT-147 symposium[34], "Computational Uncertainty in Military Vehicle Design", and (iii) experimental uncertainty quantification and test section flow characterization were significantly informed from the AVT-191 Task Group, "Application of Sensitivity Analysis and Uncertainty Quantification to Military Vehicle Design". In addition, new work to add control surface effects to the SACCON configuration aerodynamics has been established in Task Group AVT-201, "Extended Assessment of Stability and Control Prediction Methods

for NATO Air Vehicles", and preliminary results have been reported by Cummings and Schütte[35] [2014]. All of these projects have significantly benefited from the cross-project educational environment established through the STO.

B. AVT-183 Diamond Wing Project

The AVT-183 project required process development for designing the unit or combined-unit fundamental research program, computational evaluations spanning numerous numerical methods, and multiple detailed wind tunnel experiments. Consulting with the SACCON technical experts was needed, and the work was also informed by CFD-validation principles. All of these requirements were met through the STO.

Approximately 24 engineers and scientists spanning 18 organizations and 8 countries participated on this team while others provided consulting. In the course of this work, approximately 13 CFD codes were used, a new wind tunnel model was fabricated, and 4 wind tunnel tests were performed in one wind tunnel. Final reporting is underway at the time of this report, and all of this spanned about 6 years for this project.

The focus of the project was on a particular diamond wing designed to replicate the onset and progression of blunt-leading-edge vortex separation pertinent to the SACCON configuration. The diamond wing simulated some leading-edge properties of the SACCON configuration, simplified the trailing edge, and incorporated a constant airfoil section. A sketch of the diamond wing and SACCON planforms is shown in **Figure 13**. Details of this design process are given by Boelens[2] et al. [2015].

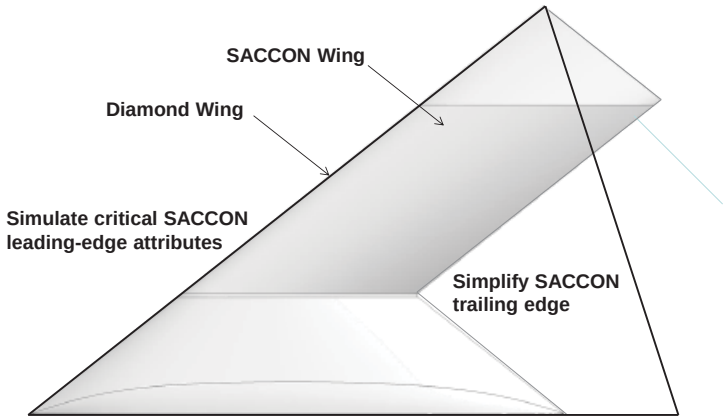

Figure 13. Diamond/SACCON concept.
Λ_{le} = 53°, $\Lambda_{te,diamond}$ = -26.5°

The studies were focused at low speeds to represent the SACCON flows and to facilitate wind tunnel experimentation. Free stream reference conditions were set at M = 0.15 and R_{mac} = 2.7 x 10^6. Angles of attack varied from 0° to 15°, and a target angle of attack of 12° was established with the vortex separation at approximately the mid leading-edge station and incipient separation flow physics upstream of this location.

In the course of the AVT-183 research program, CFD results were found to yield an incipient separation topology along with other vortical structures for the blunt-leading-edge wing that are fundamentally different from the sharp-edge wing. Some overall vortical structures were similar among the CFD predictions, while details (e.g., a separation location) differed. The wind tunnel experimentation was targeted at providing critical new data to aid in sorting out these complex vortical flows. Details of this work[2-11] will be reported in these special sessions.

From the hierarchical perspective of Figure 12, the work of AVT-183 accomplished the 'requirements flow-down' and unit problem investigation portions of the overall process. Assessments are presently underway from the unit-problem investigations for improved understanding of the blunt-leading-edge vortex separation phenomenon. The development of improved modeling of this flow from the

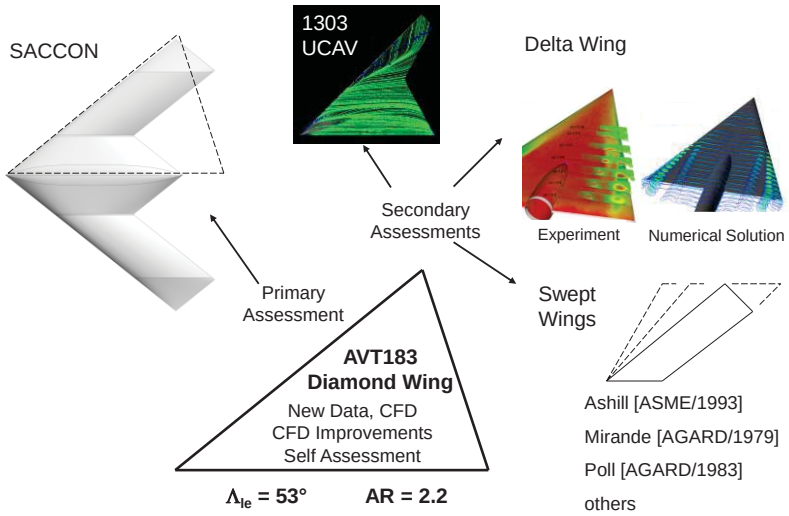

Figure 14. Computational assessments for predictive capability.

fundamental work, as well as the propagation of enhanced models up the hierarchy for performance assessments of more complex configurations, such as SACCON, is a topic for future research.

However, plans for these assessments have been established. To the extent that CFD modeling is altered, assessments can be conducted in three tiers. See **Figure 14**. The first tier is a self-assessment against the data used for the model improvement. Such assessments are necessary for model evaluation, but they are not sufficient for any predictive capability assessment. The second tier constitutes a primary predictive assessment, where models developed from the diamond wing campaign are applied to the parent SACCON configuration at relevant conditions to assess predictive improvements. The third tier constitutes secondary assessments against other relevant configurations. Plans for these include a related UCAV concept (see Petterson[36] [2006]), recent RTO results from Vortex Flow Experiment-2[32], and selected data sets from literature (e.g., Ashill[37] [1993], Mirande[38] [1979], Poll[39] [1983]). Overall recommendations for revised best practices, modelling improvements, or even model abandonment can then be sought.

VI. Concluding Remarks

A fundamental investigation of blunt-leading-edge vortical separation has been designed in such a way so that it relates to the aerodynamics of a more complex Uninhabited Combat Air Vehicle concept. The work was performed in the context of both systems level UCAV aerodynamics as well as unit-problem vortex flow investigations and principles from a hierarchical complexity approach were used to relate flow fundamentals to system-level interests.

The outcome of this process was a diamond wing configuration with a leading-edge sweep of 53° and subsequent papers include the design process details for the diamond wing as well as experimental and numerical findings. The work was coordinated through the NATO Science and Technology Organization.

VII. Acknowledgments

The work was part of a NATO/STO program entitled “Reliable Prediction of Separated Flow Onset and Progression for Air and Sea Vehicles”, also known as AVT-183. The authors appreciate the opportunity to work within the Applied Vehicle Technology (AVT) sector of the STO. The work has also been supported by a number of program and project offices. These include the NASA Revolutionary Computational Aerosciences (RCA) and the Environmentally Responsible Aircraft (ERA) projects and the NLR programmatic research funding “Kennis voor Vermogen”. All of this support is appreciated.

Finally, the authors greatly appreciate the sustained guidance from Prof. a.D. Dr.-Ing. Dietrich Hummel throughout the development and execution of the AVT-183 project.

VIII. References

[1]Cummings, R.M., Schütte, A., “Integrated Computational/Experimental Approach to Unmanned Combat Air Vehicle Stability and Control Estimation”, *AIAA Journal of Aircraft*, Vol. 49, No. 6, pp. 1542-1557, Nov-Dec 2012. (See also AIAA 2010-4392, Jun 2010).

[2]Boelens, O.J., Luckring, J.M., Breitsamter, C., Hövelmann, A., Knoth, F., Malloy, D.J., and Deck, S., “Numerical and Theoretical Considerations for the Design of the AVT-183 Diamond-Wing Experimental Investigations,” AIAA paper 2015-0062, Jan. 2015.

[3]Hövelmann, A., Knoth, F., and Breitsamter, C., “Leading-Edge Roughness Effects on the Flow Separation Onset of the AVT-183 Diamond Wing Configuration,” AIAA 2015-0063, Jan. 2015.

[4]Hövelmann, A., Grawunder, M., Buzica, A., and Breitsamter. C., “Experimental Analyses on the Flow Field Characteristics of the AVT-183 Diamond Wing Configuration,” AIAA 2015-0064, Jan. 2015.

[5]Visonneau, M., Guilmineau, E., and Toxopeus, S., “Incompressible Flow Calculations of Blunt Leading Edge Separation for a 53° Swept Diamond Wing,” AIAA paper 2015-0065, Jan. 2015.

[6]Daniel, D.T., Malloy, D.J., Reasor D.A., Jr., and Morris, C.C., “Numerical Investigations of Flow Separation on the AVT-183 53-Deg Swept Diamond Wing Configuration,” AIAA paper 2015-0066, Jan. 2015.

[7]Reasor D.A., Jr., Malloy, D.J., and Daniel, D.T., “Applicability of Hybrid RANS/LES Models in Predicting Flow Separation Onset of the AVT-183 Diamond Wing,” AIAA paper 2015-0287, Jan. 2015.

[8]Frink, N.T., “Numerical Analysis of Incipient Separation on 53° Swept Diamond Wing,” AIAA paper 2015-0288, Jan. 2015.

[9]Hitzel, S.M., Boelens, O.J., van Rooij, M., and Hövelmann, A., “Vortex Development on the AVT-183 Diamond Wing Cr9onfiguration – Numerical and Experimental Findings,” AIAA paper 2015-0289, Jan. 2015.

[10]Edefur, H., Tormalm, M., Coppin, J., Birch, T., and Nangia, R., “Numerical Study of Blunt Leading Edge Separation on a 53 Degree Swept Diamond Wing (STO AVT-183) Using the Edge and Cobalt Flow Solvers,” AIAA 2015-0290, Jan. 2015.

[11]Tomac, M., and Rizzi, A., “CFD Study of Vortex Separation Phenomena on Blunt Diamond Wing,” AIAA paper 2015-0291, Jan. 2015.

[12]Cummings, R.M., Ghoreyshi, M., Ryszka, K.J., and Lofthouse, A.J., "Vortical Flow Prediction of the AVT-183 Diamond Wing," AIAA paper 2015-0292, Jan. 2015.
[13]Anderson, J. D., Jr., *Fundamentals of Aerodynamics*, 2nd Edition, McGraw Hill, Inc., p 360, 1991.
[14]Hummel, D. On the Vortex Formation Over a Slender Wing at Large Incidence. *AGARD CP-247*, Paper 15, Jan 1979.
[15]Lambourne, N.C., and Bryer, D.W., "The Bursting of Leading Edge Vortices - Some Observations and Discussion of the Phenomenon," ARC R&M 3282, 1962.
[16]RTO, "Vortex Breakdown over Slender Delta Wings," RTO-TR-AVT-080, Oct 2009.
[17]Mitchell, A.M., "Experimental Data Base Selected for RTO/AVT Numerical and Analytical Validation and Verification: ONERA 70-Deg Delta Wing," AIAA 2003-3941, Jun 2003. (See also RTO-TR-AVT-080, Chapter 3, Oct 2009).
[18]Hall, R.M., "Impact of Fuselage Cross Section on the Stability of a Generic Fighter," AIAA 1998-2725, Jun, 1998.
[19]Miller, D.S., and Wood, R.M., "Lee-Side Flow Over Delta Wings at Supersonic Speeds," NASA TP 2430, Jun 1985
[20]Stanbrook, A., and Squire, L.C., "Possible Types of Flow at Swept Leading Edges," Aeronautical Quarterly, Vol. XV, pt. 1, Feb 1964
[21]Schiavetta, L.A., Boelens, O.J., Crippa, S., Cummings, R.M., Fritz, W., and Badcock, K.L., "Shock Effects on Delta Wing Vortex Breakdown," *AIAA Journal of Aircraft*, Vol. 46, No. 3, May-Jun 2009.
[22]Konrath, R., Klein, C., and Schroeder, A., "PSP and PIV Investigations on the VFE-2 Configuration in Sub- and Transonic Flow," AIAA 2008-379, Jan 2008
[23]Luckring, J.M., "Reynolds Number, Compressibility, and Leading-Edge Bluntness Effects on Delta Wing Aerodynamics," ICAS 04-414, Sep 2004
[24]Luckring, J.M., "A Survey of Factors Affecting Blunt Leading-Edge Separation for Swept and Semi-Slender Wings," AIAA 2010-4820, Jun 2010
[25]Hemsch, M..J., and Luckring, J.M., "Connection Between Leading-Edge Sweep, Vortex Lift, and Vortex Strength for Delta Wings," *AIAA Journal of Aircraft*, Vol. 27, No. 5, May 1990.
[26]Frink, N.T., "Strategy for Dynamic CFD Simulations on SACCON Configuration," AIAA 2010-4559, Jun 2010.
[27]Schütte, A., Hummel, D., and Hitzel, S., "Flow Physics Analysis of a Generic Unmanned Combat Aerial Vehicle Configuration", *AIAA Journal of Aircraft*, Vol. 49, No. 6, pp. 1638-1651, Nov-Dec 2012. (See also AIAA 2010-4690, Jun 2010).
[28]Oberkampf, W.L., and Trucano, T.G., "Verification and Validation in Computational Fluid Dynamics," *Progress in Aerospace Sciences*, Vol. 38, 2002
[29]Thacker, B.H., Francis, W.L., and Nicolella, D.P., "Model Validation and Uncertainty Quantification Applied to Cervical Spine Injury Assessment," RTO MP-AVT-147, Paper 26, Dec 2008.
[30]ASME. "Guide for Verification and Validation in Computational Solid Mechanics," ASME V&V 10-2006, Dec 2006.
[31]Wilson, G.E., and Boyack, B.E., "The role of the PIRT process in experiments, code development and code applications associated with reactor safety analysis," Nuclear Engineering and Design, Vol. 186, 1998.
[32]RTO. "Understanding and Modeling Vortical Flows to Improve the Technology readiness Level for Military Aircraft," RTO-TR-AVT-113, Oct. 2009.
[33]Hummel, D., and Cummings, R., *eds*, "Special Issue, VFE-2," *Aerospace Science and Technology*, Vol. 24, No. 1, 2013
[34]RTO. "Computational Uncertainty in Military Vehicle Design", RTO-MP-AVT-147, Dec 2008.
[35]Cummings, R.M., Schütte, A., "The NATO STO Task Group AVT-201 on 'Extended Assessment of Stability and Control Prediction Methods for NATO Air Vehicles'," AIAA 2014-2000. Jun 2014.
[36]Petterson, K., "CFD Analysis of the Low-Speed Aerodynamic Characteristics of a UCAV", AIAA 2006-1259, Jan 2006.
[37]Ashill, P.R., and Betts, C.J., "A Study of the Flow around the Leading Edge of a Highly-Swept Wing in a Low-Speed Wind Tunnel", ASME Engineering Conference, Jun 1993
[38]Mirande, J., Schmitt, V., and Werle, H., "Vortex Pattern Developing on the Upper Surface of a Swept Wing at High Angle of Attack", AGARD CP 247, Paper 12, Jan 1979.
[39]Poll, D.I.A., "On the Generation and Subsequent Development of Spiral Vortex Flow Over a Swept-Back Wing", AGARD CP-342, Paper 6, Jul 1983.